

Nanofabrication using neutral atomic beams

J. H. Thywissen,^{a)} K. S. Johnson, R. Younkin, N. H. Dekker, K. K. Berggren,^{b)}
A. P. Chu,^{c)} and M. Prentiss

Department of Physics, Harvard University, Cambridge, Massachusetts 02138

S. A. Lee

Department of Physics, Colorado State University, Fort Collins, Colorado 80523

(Received 9 August 1997; accepted 7 September 1997)

We present a survey of neutral atom lithography. The combination of nm-scale features, large-area parallel deposition, and effective resists demonstrates the promise of atoms as a lithographic element. We demonstrate the transfer of 70-nm-wide features from a neutral atomic beam into a substrate using several resists, including self-assembled monolayers of alkanethiolates on Au and of alkylsiloxanes on SiO₂, and “contamination” resists deposited from vapor. Unlike photons and electrons, noble gas atoms in energetic metastable states have an internal state structure that is easily manipulable, introducing the possibility of novel lithographic schemes based on the optical quenching of internal energy. © 1997 American Vacuum Society. [S0734-211X(97)00706-3]

I. INTRODUCTION

Neutral atom lithography uses a patterned neutral atomic beam to create permanent structures on surfaces. In this article, we provide an introduction to neutral atom lithography intended for readers unfamiliar with atom optics; furthermore, we present an overview of our recent lithography work. For a more detailed treatment, we refer the reader to the listed references and reviews.

Neutral atoms offer several attractive properties for lithography. Neutral atomic beams are simple and inexpensive sources of particles with kinetic energies < 1 eV and de Broglie wavelengths < 1 Å. The trajectories of neutral atoms are unaffected by uniform electric or magnetic fields, and the long-range interparticle forces between neutral atoms are small. A variety of atom optical elements—masks, lenses, lens arrays, mirrors, waveguides, beam splitters, and holograms—has been demonstrated.¹ Lens arrays^{2–6} have allowed the parallel deposition of periodic structures with < 15 -nm-wide features, and can produce excellent registration over large areas.⁷

Neutral atomic beams offer a degree of freedom that is not available in electron or photon beams: atoms can have laser-accessible internal state structure. This internal structure permits several desirable manipulations: (1) laser cooling⁸ can be used to enhance the flux and collimation of atomic beams; (2) a noble gas atom in a metastable excited state⁹ can carry 8–20 eV of internal energy, which can be delivered to a surface without penetrating more than a few Å into the bulk material; (3) dissipation of the atom’s internal energy can be initiated by a single IR photon.

In the following sections, we will survey a variety of atom optics that has been demonstrated (Sec. II); discuss standing wave focusing and deposition onto a substrate (Sec. III); re-

port on recent experiments in which resists sensitive to atoms have been developed (Sec. IV); and present novel patterning schemes based on the manipulation of internal states (Sec. V). We also include an Appendix on typical neutral atomic beams and sources.

II. ATOM OPTICS

A. Atom optics based on micro-fabricated masks

Atoms with kinetic energies ≤ 1 eV do not pass freely through materials, so $\sim \mu\text{m}$ -thick Si₃N₄ membranes form excellent masks for atomic beams. Transmission masks for atoms must be stencil masks, i.e., self-supporting and free standing, which limits the geometries available. Fresnel lenses,^{10–12} diffractive beam splitters,^{13,14} amplitude holograms,¹⁵ near field optics,¹⁶ and contact masks for neutral atoms have been constructed from micro- and nanofabricated material masks.

Of these fabricated elements, only contact masks have been used in atom lithography. The diffraction limit on the minimum feature size is $\sim \sqrt{\lambda_{\text{dB}} D}$, where λ_{dB} is the de Broglie wavelength of the atom (≤ 1 Å) and D is the separation between the mask and the substrate. Thus for a mask $5 \mu\text{m}$ from the surface and atoms with a 0.1 Å wavelength, ~ 7 -nm-wide features are the smallest allowed by diffraction.

B. Atom optics based on magnetic fields

Unlike charged particles, neutral atoms are not deflected by spatially uniform magnetic fields; however, most atoms have an intrinsic magnetic moment μ , typically on the order of a Bohr magneton. The energy of a magnetic dipole in a magnetic field $\mathbf{B}(\mathbf{r})$ is $U(\mathbf{r}) = -\mu(\mathbf{r}) \cdot \mathbf{B}(\mathbf{r})$, so the force on an atom is proportional to the gradient of the field. Lenses^{17,18} and mirrors¹⁹ have been created using the magnetic fields from permanent magnets.

Kaenders *et al.* have demonstrated a projection lens system for atoms;¹⁸ such a magnetic lens might be used to image atoms onto a substrate. The focal length of a thin lens for

^{a)}Electronic mail: joseph@atomsun.harvard.edu

^{b)}Current address: Analog Device Technology Group, MIT Lincoln Laboratories, Lexington, MA 02173.

^{c)}Current address: Lehman Brothers, 3 World Financial Center, NY, NY 10285.

atoms is proportional to v_L^2/β , where v_L is the longitudinal velocity of the atom and β is the curvature of the focusing potential. Gradients of up to ~ 1 T/cm were used in these magnetic lenses to accelerate Cs atoms at $\sim 4 \times 10^5$ m/s². A magnetic hexapole lens with $f = 10$ cm has been demonstrated with a Cs beam at $v_L = 70$ m/s. The diffraction-limited spot size at the focus of a thin lens with focal length f and input beam size D is

$$\delta x \sim f \lambda_{dB} / D. \quad (1)$$

For the lens described above, assuming $D = 1$ mm, Eq. (1) predicts $\delta x \sim 1$ nm. However, when the aberrations of this lens are taken into account, a focal spot size of 50 nm is predicted to be possible.

C. Atom optics based on laser light

Although many atoms possess intrinsic magnetic dipole moments, the intrinsic electric dipole moment in a neutral atom is zero. However, an electric field can induce a dipole moment \mathbf{P}_{ind} in the neutral atom. For an electric field $\mathbf{E}(\mathbf{r})$ that oscillates at a frequency ω far from an atomic resonant frequency ω_0 , the induced dipole moment $\mathbf{P}_{ind}(\mathbf{r})$ is small. For an electric field oscillating at a frequency ω near ω_0 , as can be the case for optical frequencies, the induced dipole moment can have an amplitude of the order of a Debye, where the amplitude of \mathbf{P}_{ind} is resonantly enhanced and increases with the field amplitude.

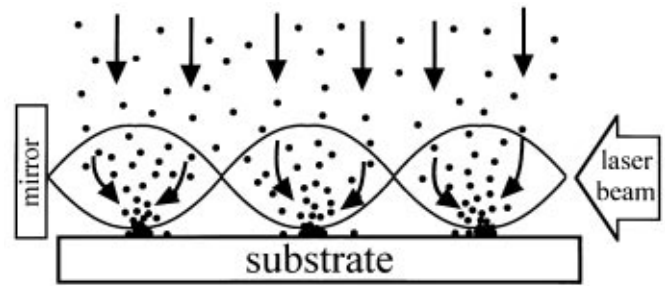
For $\omega < \omega_0$, the induced dipole moment is parallel to the electric field, so the energy of the dipole $U(\mathbf{r}) = -\mathbf{P}_{ind} \times (\mathbf{r}, \omega) \cdot \mathbf{E}(\mathbf{r})$ is a minimum where the laser intensity is a maximum. For $\omega > \omega_0$, the induced dipole is antiparallel to the field, so the energy is a minimum at the intensity minimum.²⁰

The light potential has been used to create various atom optical elements including lenses,^{21–23} lens arrays,^{2–6} mirrors,^{24–27} beam-splitters,^{28–30} and waveguides.^{31–33}

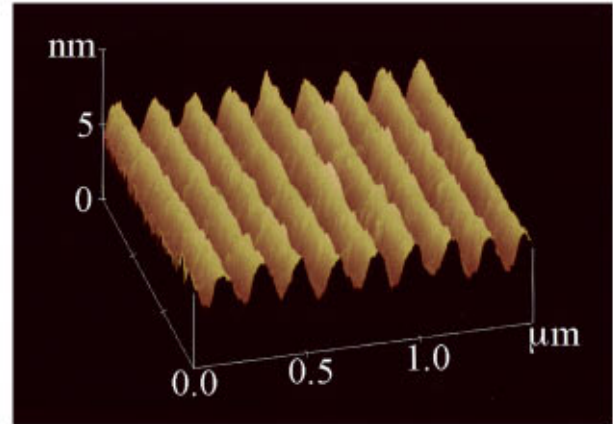
For instance, Sleator *et al.*²² created a lens with a single potential minimum at an antinode of a large-period standing wave³⁴ of laser light with $\omega < \omega_0$. The focal length of this thin lens scales as $v_L^2 \lambda_{eff}^2 / I_0^{1/2}$, where I_0 is the peak laser intensity and λ_{eff} is the effective wavelength of the standing wave. For metastable helium (He*) with $v_L = 1800$ m/s, $D = 25 \mu\text{m}$, $\lambda_{eff} = 45 \mu\text{m}$, and $f = 57$ cm, the observed spot size reached the diffraction limit predicted by Eq. (1) of $2 \mu\text{m}$. Atoms were accelerated as quickly as $\sim 10^6$ m/s² during their 40 ns of interaction with the laser light.

III. DIRECT DEPOSITION VIA STANDING WAVE FOCUSING

An intense standing wave of near-resonant laser light can be used to form a periodic array of lenses for atoms. Lens arrays are lithographically interesting because (1) the high field gradients can create lenses with focal lengths of $\sim 50 \mu\text{m}$ and can focus atoms into sub-100-nm-wide features; (2) an array of lenses enables the parallel deposition of these nm-scale features; and (3) the use of a coherent laser provides precise registration.



(a)



(b)

FIG. 1. Standing waves of laser light have been used as an array of cylindrical lenses to focus atoms during deposition onto substrates. (a) Schematic representation of standing-wave focusing. (b) Atomic force microscopy image of Al lines formed using the technique depicted in (a). The lines are spaced by 155 nm, and the feature width is approximately 70 nm.

A. Standing wave lens arrays

An array of lenses can be created with two counterpropagating beams of light that interfere to form a standing wave intensity distribution [see Fig. 1(a)]. As explained above, the atoms experience a force towards the intensity antinodes (for $\omega < \omega_0$) and thereby are focused onto the underlying substrate. Lenses with focal lengths of $\sim 50 \mu\text{m}$ and accelerations of $\sim 3 \times 10^7$ m/s² can be obtained for peak laser intensities I_0 of 10^5 mW/cm².

The standing wave lenses in the arrays described here are thick lenses, so the atoms move significantly while in the lens. The focal length scales as $v_L I_0^{-1/2}$; for Na traveling at 650 m/s into a $\lambda/2$ diameter lens with $f \sim 50 \mu\text{m}$, Eq. (1) predicts the diffraction-limited spot size $\delta x \approx 2$ nm. In practice, lens aberrations and other feature-broadening mechanisms have limited the feature sizes to > 10 nm; these mechanisms will be discussed in Sec. III C.

B. Direct deposition experiments

In the first neutral atom lithography experiment employing the laser manipulation of atoms, a cylindrically focused laser beam acted as a “stencil” to pattern a Na beam.²³ A 150- μm -wide Na feature was deposited on an underlying substrate.

In demonstrations of the first *nanolithography* using atom optics, Timp *et al.* used an optical standing wave to focus an atomic Na beam into an array of features spaced by half an optical wavelength. Experimental extensions and improvements have created <15-nm-wide Na lines spaced 295 nm apart.² Standing wave focusing experiments have also created Cr gratings with 40-nm-wide features spaced 213 nm apart^{3,5} and Al gratings with 70-nm-wide features and a 155 nm periodicity⁴ [see Fig. 1(b)]. Finally, three- and four-beam interference patterns have produced two-dimensional arrays of Cr features with ~ 100 nm widths and ~ 200 nm spacings.³⁵

Atomic deposition through a standing wave lens array replicates the positions of the nodes of an optical interference pattern. These replicas can, in principle, have excellent registration over large areas ($\sim 3 \times 10^4$ mm²).⁷ Lithography using interfering optical fields has been demonstrated for use as a length standard,³⁶ direct deposition through a standing wave shares the same advantages and might also have applications as a length standard for lithography or microscopy.

C. Feature size and background height

The contributions to feature size and background height have been studied extensively, both theoretically³⁷ and experimentally.²

Lens aberrations include chromatic and spherical aberrations. Near its minima, the optical potential formed by a standing wave is approximately parabolic. Atoms near these minima undergo harmonic motion with an oscillation time T_{osc} , such that atoms with no transverse velocity and longitudinal velocity v_L will come to a focus after a distance of $v_L T_{\text{osc}}/4$. Typical atomic beams contain a spread of velocities v_L (see the Appendix on sources), so atoms would be focused at a variety of distances; this aberration is analogous to chromatic aberrations in optical lenses, where photons with different wavelengths propagate with different phase velocities in the lens medium. In addition, standing wave lenses suffer from spherical aberrations, as a sinusoidal potential is no longer parabolic far from its minima. These aberrations do not significantly broaden the features, but they do result in a pedestal around the feature.³⁸

Even for an ideal lens, a nonzero transverse velocity distribution can limit the size of the focused spot. This velocity spread has limited the size of the smallest features formed to date with standing wave focusing.² The chromatic³⁹ and spherical⁴⁰ aberrations discussed above contribute to an increased background, which typically limits the feature height to background ratio to $\sim 10:1$.

IV. ATOM LITHOGRAPHY WITH RESISTS

Many of the atoms that are easily manipulated with atom optics are either highly reactive or volatile, so they are not suitable for the creation of durable, permanent structures using direct-deposition lithography; consequently, we have developed resists that are sensitive to several species of neutral atoms. Incorporating resists into neutral atom lithography provides several advantages: (1) fabrication in a variety of

materials—resists allow patterns created in technologically uninteresting particles (e.g., metastable noble gases and alkali metals) to be transferred to a variety of technologically relevant materials (e.g., coinage metals, semiconductors, and dielectric insulators); (2) feature height amplification—sensitive resists and selective etching allow the possibility to create tall structures (tens of nm) using low atomic doses (monolayers); (3) contrast enhancement—nonlinearities in the transfer function of the resist/etch should bring more flexibility and better performance to the atom lithographic techniques already demonstrated. Ultrathin resists have been demonstrated to have both a high sensitivity to neutral atoms and a high resolution. These resists fall into two classes: self-assembled monolayers (SAMs) of organic molecules, and materials deposited onto a surface from background vapor.⁴¹ SAMs have been patterned both by alkali metals and metastable noble gas atoms; lithography with a vapor-deposited resist has been demonstrated using several species of metastable atoms as patterning agents.

A. SAM resists sensitive to alkali metals

Alkali atoms have patterned both alkanethiolate SAMs on gold films^{42,43} and alkylsiloxane SAMs on SiO₂ layers.⁴⁴

Alkanethiolate SAMs exposed to a beam of neutral Cs atoms patterned by a physical mask produced ~ 70 -nm-wide features.⁴² The atomic Cs beam was patterned using a contact mask consisting of a $40 \mu\text{m} \times 40 \mu\text{m}$ Si₃N₄ membrane perforated with 50-nm and 0.5- μm -scale holes. After exposure to greater than three Cs atoms per molecule of the SAM (1.5×10^{15} atoms/cm², or 10 min for the parameters of our beam), the SAM was sufficiently altered by the atomic beam that a subsequent wet-chemical etch could be used to transfer positive-tone features as small as 70 nm wide into the underlying Au. An investigation of the response of the resist/etch system versus dose showed that a critical dose for damage occurred at ~ 3 atoms per SAM molecule, followed by a region of linear response, and then saturation.

A recent experiment by the Meschede group used an optical standing wave to focus an atomic Cs beam onto a thiolate SAM; the pattern formed in the SAM was again transferred into the underlying Au substrate by wet-chemical etching.⁶

In our experiments, the edge resolution of the features created using Cs to pattern SAMs on Au seemed to be limited by the grain size of the Au films, so we instead used alkylsiloxane SAMs formed on an amorphous substrate of SiO₂. Using a similar Si₃N₄ mask, we were able to form ~ 70 -nm-wide features in Si with ~ 10 atoms per SAM molecule. The pattern in the SAM was transferred to the thin (1–2 nm-thick) SiO₂ surface layer and then into the underlying Si using a two-step wet-chemical etch.⁴⁴ We do not yet understand the mechanism by which neutral Cs atoms can alter the SAMs. However, we have seen that SAMs on both Au and SiO₂ substrates can be patterned, suggesting that alkali atoms may be able to damage SAMs formed on other materials as well.^{45–47}

B. Resists sensitive to metastable noble gas atoms

A noble gas atom with ~ 50 meV of kinetic energy cannot be used to damage or modify a resist because noble gas atoms are not chemically reactive. Noble gas atoms in a metastable excited state,⁹ however, are de-excited upon interaction with a substrate and dissipate their 8–20 eV of internal energy into the surface. Secondary electrons in this energy range have a mean free path in the substrate of only a few angstroms;⁴⁸ the energy dissipation of the metastable is therefore probably localized to a radius of a few angstroms. This situation is ideal for lithography: these massive, thermal atoms have a wavelength roughly equal to that of hard x rays or ~ 10 keV electrons, and yet they deposit their energy in the surface layer without damaging the underlying material.

1. Self-assembled monolayers

It has been demonstrated that a resist of alkanethiolate SAMs formed on Au can be patterned with metastable argon (Ar^*) atoms.^{49,50} The energy dissipated when the metastable atoms are de-excited causes a change in the SAM sufficient to allow penetration by a wet-chemical etch. Exposing the SAM to an atomic Ar^* beam through a copper grid yielded an edge resolution of < 100 nm.

Metastable helium was also used to damage a SAM layer.^{51,52} Roughly ten times more Ar^* than He^* atoms are required to damage a SAM, even though the energy stored in He^* (20 eV) is only about twice that stored in Ar^* (12 eV).^{50,53} Typical doses of He^* atoms required to damage a SAM range from ~ 0.3 to 2 atoms per SAM molecule ($\sim 1 \times 10^{15}$ atoms/cm²) during 5–20 min exposures. Assuming all the energy stored in the He^* atoms is transferred into the surface, this corresponds to an energy dose of ~ 3 mJ/cm².

2. Contamination deposition

In the presence of dilute hydrocarbon background vapors (diffusion pump oil), metastable atoms can assist in the formation of a durable carbonaceous material. This material can subsequently be used as a mask against a variety of etching techniques in a negative-tone process. Although our demonstrations have used the residual vapor due to the diffusion pump oil, we expect that metastable-assisted deposition from a vapor may be a more widely applicable technique, either to deposit a carefully engineered vapor precursor, to activate chemical reactions, or to mediate *in situ* growth.

In our laboratory, we have used Ar^* and contamination lithography to create ~ 70 nm wide nanostructures in Au, Si, and SiO_2 .⁵⁴ Figure 2 shows features etched in Si following exposure to $\sim 2 \times 10^{16}$ atoms/cm² (16 h); this corresponds to ~ 40 mJ/cm² of deposited energy, resulting in a ≤ 5 -nm-thick layer of material. After exposure, the sample was etched first in 1% aqueous HF to pattern the SiO_2 layer and then in 40% aqueous KOH to transfer the pattern into the Si. With increased atomic flux, we have created nm-scale features using 1×10^{16} atoms/cm² in just one hour of exposure; further enhancements in beam flux are achievable.⁵⁵ In order to demonstrate the potential parallelism of neutral atom lithography,

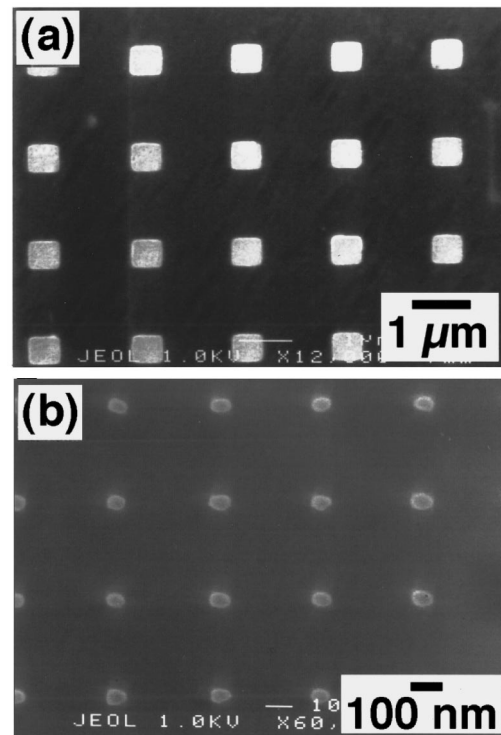


FIG. 2. Scanning electron microscopy images of nm-scale features created in Si (110) using metastable argon and contamination lithography. The patterns were created by exposing the substrate through a perforated Si_3N_4 membrane in the presence of a background siloxane vapor and using the deposited film as a resist against a wet-chemical etching. (a) and (b) correspond to regions of the mask with $0.5\text{-}\mu\text{m}$ -square and ~ 50 -nm-round perforations, respectively.

we have also used an Ar^* beam to pattern simultaneously an entire 3 in. SiO_2 wafer masked by a stainless steel mesh.⁵⁴

In a subsequent set of experiments on atomic contamination lithography, metastable neon (17 eV) was used to deposit carbon material onto GaAs substrates.⁵⁶ The GaAs substrates were etched with an anisotropic chemically assisted ion beam etching technique, yielding the highest aspect ratio features produced in neutral atom lithography: 50-nm-diam features more than 100 nm tall were produced using a physical mask to pattern the atomic beam. These Ne^* experiments were performed using an oil vapor and atomic beam apparatus distinct from the Ar^* experiments, indicating that the precise nature of the background vapor is not critical to the process.

V. INTERNAL STATE PATTERNING TECHNIQUES

Metastable argon has an internal state structure that allows laser light to de-excite the metastable atoms in a process called “quenching:” first, the atom is excited by an IR laser photon from the metastable state to a less stable atomic state. The atom can then radiatively decay from this further excited state to the atomic ground state. In this multiple-step radiative decay process, the energy (12 eV) stored in the metastable state is dissipated as a UV photon. We have

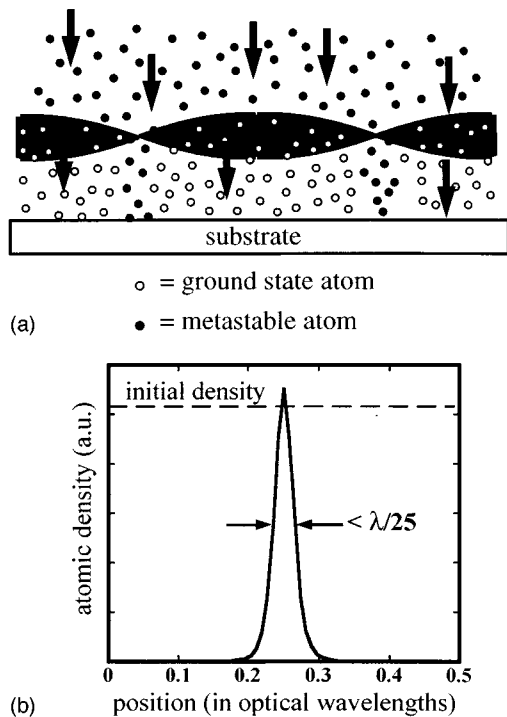


FIG. 3. (a) Schematic representation of standing-wave quenching. Only in the nodes of the standing wave do the atoms remain in the metastable state—elsewhere, they are quenched. The remaining metastable atoms can be used either to damage a SAM resist or to form a contamination resist. (b) Results of a quantum calculation for the position distribution of metastable atoms transmitted near the node of the standing wave; this calculation includes realistic atomic beam and laser beam parameters. Localizations of $\lambda/25$ or 30 nm should be possible for Ar*. (See Ref. 57 for details.)

shown that the decay process converts an atom in an energetic excited state, which can expose the resist, into an atom in the ground state, which does not expose the resist.^{49,54} These experiments introduce a novel type of patterning technique for lithographic applications: instead of physically moving or masking the atoms, the internal state of the atom is modified in a position-dependent way.

A. Standing-wave quenching

A standing-wave laser field resonant with the quenching transition is a simple, specific example of a spatially dependent quenching geometry that may be used to form nm-scale patterns in atom lithography.^{57–59}

The laser frequency and intensity can be chosen so that the atoms will be quenched rapidly everywhere except in very narrow regions around the nodes. Metastable atoms passing through these low intensity regions will retain their internal energy until they hit the substrate [Fig. 3(a)]. At positions where atoms are excited with high probability (far from the nodes), the population decays exponentially in time, leading to extremely high contrast between transmission in quenched and unquenched regions. When the laser frequency is detuned above the atomic resonance, the mechanical effects of the standing wave confine the atoms near the nodes; therefore, the surviving atomic distributions can approach the ground state of the confining optical potential well. The

standing wave acts as an absorptive grating for the atoms; the degree of localization and the diffraction pattern produced by such a grating have been examined theoretically.^{57,58} Figure 3(b) shows the results of a quantum Monte Carlo calculation of the position distribution around one node of a standing wave. For a 100 mW laser beam 1 mm wide and a realistic atomic Ar* beam velocity profile, the width of the distribution of metastables approaches $\lambda/25$, or ~ 30 nm.⁵⁷

The effect of this standing-wave absorptive grating is quite different from the focusing with a standing light wave. Whereas in the focusing case, the light acts as a lens, in the quenching case, the light more closely resembles a lossy waveguide. The quenching light forms a potential that confines the atoms near the nodes of the standing wave, and the quantum mechanical modes of that potential well that are most localized are quenched least rapidly. Thus, the ultimate limit for this technique is the width of the lowest energy mode of the light-induced potential well, and the process acts to select only the atoms in this mode by quenching all others. In the case of focusing, atoms populate many modes of the well and the degree of localization, in the absence of aberrations, is limited by the amount of transverse momentum that can be imparted to the atom by the light field. The minimum feature size in these two processes scales differently with the laser intensity: the quenching feature size goes as $I^{-1/4}$, the focusing, as $I^{-1/2}$. However, the very different physical processes lead to different trade offs with respect to various aberrations, source properties, viable atoms, and the area of the resulting pattern. For instance, in the case of a thermal beam, the peak-to-background density ratio in quenching is predicted to be 1000:1, as compared to the 10:1 typical of standing-wave focusing.⁵⁷

Standing waves resonant with the quenching transition have been used to pattern a substrate with large-scale features. Passing a beam of atoms through a large-period (400 μm) optical standing wave³⁴ produced 125- μm -wide damaged regions in a SAM,⁵¹ demonstrating the narrowing expected due to the nonlinearities in the atom/field system and the quenching process.

The simple standing wave can be generalized to a two-dimensional interference pattern to produce a periodic array of dots. Since this quenching technique depends only on the presence and absence of light, if one could create an arbitrary intensity/nodal pattern in light, this pattern could be transferred to the atomic beam and subsequently into a substrate.⁵⁰

B. Using external potentials for more complex patterning

In addition to the position-dependent quenching caused by the intensity variation in a standing wave, other schemes are under investigation that might be used to achieve spatially dependent distributions of metastable atoms. For instance, an externally applied potential (e.g., a light-induced potential or static electromagnetic field gradient) could be used to produce a position dependent shift in the atomic

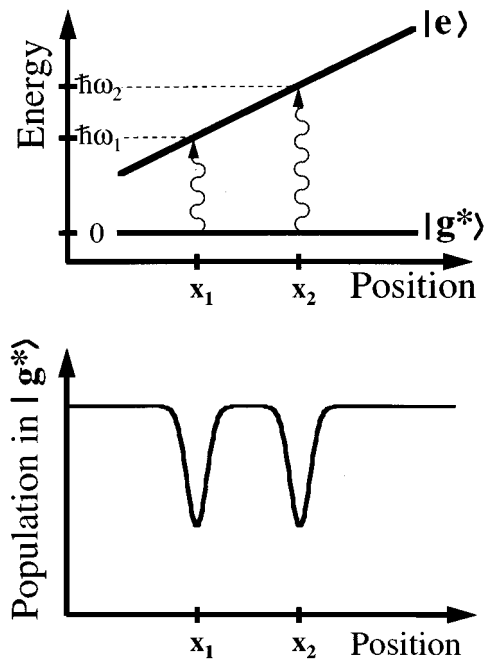


FIG. 4. An externally applied potential can produce a position-dependent shift in the atomic transition frequency between the metastable state $|g^*\rangle$ and the further excited state $|e\rangle$. This position dependence allows a spatially uniform probe laser to induce transitions between atomic energy levels at specific positions, which depend on the frequencies of the probe lasers. Multiple probes with different frequencies (ω_1 and ω_2) can be used to transfer population at a variety of positions (x_1 and x_2) simultaneously. If this population transfer quenches metastable atoms, the technique might be used for lithography.

resonant frequency, $\omega_0(x)$. A spatially uniform probe beam at frequency ω would then only excite atoms near the position in space where $\omega_0(x) = \omega$. Probe beams of different frequencies could be used to simultaneously quench atoms at a variety of positions. Thomas *et al.*^{60,61} have pioneered such a technique for measuring and inducing localized position distributions in atomic beams, but their methods have yet to be applied to nanofabrication.

Figure 4 shows how this scheme can be used to create more arbitrary distributions in the population of metastable atoms. An external field gradient shifts the energy of the excited state, $|e\rangle$, such that two spatially uniform probe lasers, of frequencies ω_1 and ω_2 , induce transitions in narrow regions around positions x_1 and x_2 . The widths of the features are limited by the potential gradients achievable, the diffraction of the atoms, and the velocity spread of the atomic beam. Theoretical simulations suggest that, with achievable source and laser parameters, schemes based on these ideas could produce features smaller than 10 nm.⁶²

VI. SUMMARY

We have presented a survey of neutral atom lithography and an overview of our recent work in the field. Recent developments in atom optics have made possible the manipulation and patterning of neutral atom beams. The combination of nm-scale features, large-area parallel deposition, and excellent registration has demonstrated the promise of atoms

as a lithographic element. Unlike photons and electrons, atoms have an internal state structure that is easily manipulated. We have developed resists that are sensitive to neutral atoms and that make possible not only traditional etching techniques, but also novel lithographic schemes based on the optical quenching of internal energy.

ACKNOWLEDGMENTS

This work was supported in part by NSF Grant No. PHY 9312572, and made use of the Harvard MRSEC shared facilities. We would like to thank our collaborators A. J. Black, E. Cheung, D. M. Giltner, R. W. McGowan, M. Ol'shanii, D. C. Ralph, H. Robinson, S. P. Smith, G. M. Whitesides, and J. L. Wilbur for their contributions. J.H.T. acknowledges the Fannie and John Hertz Foundation. K.S.J. acknowledges an AT&T/Lucent Technologies PhD fellowship. A.P.C. acknowledges a NSF Graduate Fellowship.

APPENDIX: SOURCES

Standard sources for beams of neutral atoms⁶³ include thermal and jet sources with less than 100 meV of kinetic energy. In this Appendix, we present two specific examples of neutral atomic beams that have been used for atomic lithography. This provides the context for understanding practical limitations on feature size and deposition time.

1. Thermal sources

The simplest source for atoms is a thermal source, in which atoms in thermal equilibrium with the walls of a container effuse through a small (mm-scale) hole. The velocity distribution of the effused atoms has a width that is approximately equal to the most probable velocity, v_{mp} . In our thermal Cs source, for example, at 150 °C, $v_{mp} = 280$ m/s, the kinetic energy is 53 meV, and the flux is $\sim 4 \times 10^{12}$ atoms $\text{cm}^{-2} \text{s}^{-1}$; at 300 °C the flux has increased to 7×10^{14} atoms $\text{cm}^{-2} \text{s}^{-1}$, but the other parameters are almost unchanged. Sources for other elements, such as Cr and Al, require significantly higher temperatures to achieve the same flux. For instance, an Al beam⁴ at 1400 °C has a flux of $\sim 2 \times 10^{14}$ atoms $\text{cm}^{-2} \text{s}^{-1}$.

The advantage of a thermal source is that the beam flux is proportional to the vapor pressure, which increases exponentially with temperature. However, the broad longitudinal velocity spread of a thermal source distribution is unacceptable for applications such as interferometry and holography. Velocity selection or cooling⁵⁵ can decrease the width of the atomic velocity distribution. The velocity width of alkali beams can also be made smaller by seeding them into a supersonic expansion of an inert gas.⁶⁴

2. Metastable dc discharges

A noble gas atom can be excited to a long-lived "metastable" state⁹ which has an energy of 8–20 eV. One excitation technique^{65,66} uses a needle at a discharge voltage (~ 1 kV) to create a plasma at the aperture of a high pressure

source. Typical plasmas produce one metastable per 10^4 to 10^5 ground state atoms.⁶⁵ For example, our Ar* beam has a source pressure of ~ 100 Torr, resulting in $v_{mp} \sim 800$ m/s and a flux of 3×10^{12} atoms $\text{cm}^2 \text{s}^{-1}$ at a substrate 35 cm from the source.⁶⁷

Unlike alkali sources, whose flux can be increased simply and dramatically by increasing the source temperature, the nature of the plasma puts a significant constraint on the metastable flux that can be achieved. However, parallel source geometries and/or beam brightening techniques may result in significant flux enhancement.⁵⁵

¹For a review of atom optics and optical forces, see C. S. Adams, M. Sigel, and J. Mlynek, *Phys. Rep.* **240**, 143 (1994), and references therein.

²G. Timp, R. E. Behringer, D. M. Tennant, J. E. Cunningham, M. Prentiss, and K. K. Berggren, *Phys. Rev. Lett.* **69**, 1636 (1992); R. E. Behringer, V. Natarajan, G. Timp, and D. M. Tennant, *J. Vac. Sci. Technol. B* **14**, 4072 (1996); V. Natarajan, R. E. Behringer, and G. Timp, *Phys. Rev. A* **53**, 4381 (1996).

³J. J. McClelland, R. E. Scholten, E. C. Palm, and R. J. Celotta, *Science* **262**, 877 (1993); R. Gupta, J. J. McClelland, Z. J. Jabbour, and R. J. Celotta, *Appl. Phys. Lett.* **67**, 1378 (1995).

⁴R. W. McGowan, D. M. Giltner, and S. A. Lee, *Opt. Lett.* **20**, 2535 (1995).

⁵U. Drodofsky, J. Stuhler, B. Brezger, Th. Schulze, M. Drewsen, T. Pfau, and J. Mlynek, *Microelectron. Eng.* **35**, 285 (1997).

⁶D. Meschede, presented at the Atom Optics conference at Optoelectronics '97, San Jose, CA, 1997.

⁷R. E. Behringer, V. Natarajan, and G. Timp, *Appl. Phys. Lett.* **68**, 1034 (1996).

⁸For a review of laser cooling and trapping see H. Metcalf and P. van der Straten, *Phys. Rep.* **244**, 203 (1994), and references therein.

⁹The metastable rare gas atoms have the following energies: He* = 20 eV, Ne* = 17 eV, Ar* = 12 eV, Kr* = 10 eV, and Xe* = 8 eV. Their natural lifetimes are ≥ 20 ms, which is much longer than their typical flight times.

¹⁰N. P. Bigelow, M. G. Prentiss, D. Tennant, J. E. Bjorkholm, and M. O'Malley, QELS 1990.

¹¹O. Carnal, M. Sigel, T. Sleator, H. Takuma, and J. Mlynek, *Phys. Rev. Lett.* **67**, 3231 (1991).

¹²C. R. Ekstrom, D. W. Keith, and D. E. Pritchard, *Appl. Phys. B* **54**, 369 (1992).

¹³D. W. Keith, C. R. Ekstrom, Q. A. Turchette, and D. E. Pritchard, *Phys. Rev. Lett.* **66**, 2693 (1991).

¹⁴O. Carnal, A. Faulstich, and J. Mlynek, *Appl. Phys. B* **53**, 88 (1991).

¹⁵M. Morinaga, M. Yasuda, T. Kishimoto, and F. Shimizu, *Phys. Rev. Lett.* **77**, 802 (1996).

¹⁶J. F. Clauser and S. Li, *Phys. Rev. A* **44**, R2213 (1994); O. Carnal, Q. A. Turchette, and H. J. Kimble, *ibid.* **51**, 3079 (1995); M. S. Chapman, C. R. Ekstrom, T. D. Hammond, J. Schmiedmayer, B. E. Tannian, S. Wehinger, and D. E. Pritchard, *ibid.* **51**, R14 (1995).

¹⁷H. Friedberg and W. Paul, *Naturwissenschaften* **38**, 159 (1951); H. Friedberg, *Z. Phys.* **130**, 493 (1951).

¹⁸W. G. Kaenders, F. Lison, A. Richter, R. Wynands, and D. Meschede, *Nature (London)* **375**, 214 (1995); W. G. Kaenders, F. Lison, I. Müller, A. Richter, R. Wynands, and D. Meschede, *Phys. Rev. A* **54**, 5067 (1996).

¹⁹G. I. Opat, S. J. Wark, and A. Cimmino, *Appl. Phys. B* **54**, 396 (1992); T. M. Roach, H. Abele, M. G. Boshier, H. L. Grossman, K. P. Zetie, and E. A. Hinds, *Phys. Rev. Lett.* **75**, 629 (1995); A. I. Sidorov, R. J. McLean, W. J. Rowlands, D. C. Lau, J. E. Murphy, M. Walkiewicz, G. I. Opat, and P. Hannaford, *Quantum Semiclass. Opt.* **8**, 713 (1996).

²⁰For a more complete explanation and review of laser manipulation of neutral atoms, see S. Stenholm, *Eur. J. Phys.* **9**, 242 (1988); A. Aspect, R. Kaiser, N. Vansteenkiste, and C. I. Westbrook, *Phys. Scr.* **T58**, 69 (1995).

²¹J. E. Bjorkholm, R. R. Freeman, A. Ashkin, and D. B. Pearson, *Phys. Rev. Lett.* **41**, 1361 (1978).

²²T. Sleator, T. Pfau, V. Balykin, and J. Mlynek, *Appl. Phys. B* **54**, 375 (1992).

²³M. Prentiss, G. Timp, N. Bigelow, R. E. Behringer, and J. E. Cunningham, *Appl. Phys. Lett.* **60**, 1027 (1992).

²⁴R. J. Cook and R. K. Hill, *Opt. Commun.* **43**, 258 (1982).

²⁵V. I. Balykin, V. S. Letokhov, Yu. B. Ovchinnikov, and A. I. Sidorov, *Phys. Rev. Lett.* **60**, 2137 (1988).

²⁶M. A. Kasevich, D. S. Weiss, and S. Chu, *Opt. Lett.* **15**, 607 (1990).

²⁷C. G. Aminoff, A. M. Steane, P. Bouyer, P. Desbiolles, J. Dalibard, and C. Cohen-Tannoudji, *Phys. Rev. Lett.* **71**, 3083 (1993).

²⁸M. Kasevich and S. Chu, *Phys. Rev. Lett.* **67**, 181 (1991).

²⁹P. L. Gould, G. A. Ruff, and D. E. Pritchard, *Phys. Rev. Lett.* **56**, 827 (1986).

³⁰J. Lawall and M. Prentiss, *Phys. Rev. Lett.* **72**, 993 (1994).

³¹V. I. Balykin, V. S. Letokhov, Yu. B. Ovchinnikov, A. I. Sidorov, and S. V. Shul'ga, *Opt. Lett.* **13**, 958 (1988).

³²M. J. Renn, D. Montgomery, O. Vdovin, D. Z. Anderson, C. E. Wieman, and E. A. Cornell, *Phys. Rev. Lett.* **75**, 3253 (1995).

³³H. Ito, T. Nakata, K. Sakaki, M. Ohtsu, K. I. Lee, and W. Jhe, *Phys. Rev. Lett.* **76**, 4500 (1996).

³⁴A large-period standing wave can be created by interfering two laser beams at \sim mrad angles.

³⁵R. Gupta, J. J. McClelland, Z. J. Jabbour, and R. J. Celotta, *Appl. Phys. Lett.* **67**, 1378 (1995); U. Drodofsky, J. Stuhler, Th. Schulze, M. Drewsen, B. Brezger, T. Pfau, and J. Mlynek, *Appl. Phys. B* (to be published).

³⁶J. Ferrera, M. L. Schattenburg, and Henry I. Smith, *J. Vac. Sci. Technol. A* **14**, 4009 (1996).

³⁷J. J. McClelland and M. R. Scheinfein, *J. Opt. Soc. Am. B* **8**, 1974 (1991); K. K. Berggren, M. Prentiss, G. L. Timp, and R. E. Behringer, *J. Opt. Soc. Am. B* **11**, 1166 (1994).

³⁸The spread in longitudinal velocities makes the deposition relatively insensitive to the separation between the substrate and standing wave.

³⁹An achromatic lens geometry is analyzed in M. Drewsen, R. J. C. Spreeuw, and J. Mlynek, *Opt. Commun.* **125**, 77 (1996).

⁴⁰A standing-wave lens geometry with less spherical aberration is analyzed in M. K. Olsen, T. Wong, S. M. Tan, and D. F. Walls, *Phys. Rev. A* **53**, 3358 (1996).

⁴¹Electron beam lithography has demonstrated that both SAMs and contamination lithography are capable of supporting < 10 nm features. See M. J. Lercel, H. G. Craighead, A. N. Parikh, K. Seshadri, and D. L. Allara, *Appl. Phys. Lett.* **68**, 1504 (1996); A. N. Broers, W. W. Molzen, J. J. Cuomo, and N. D. Wittels, *ibid.* **29**, 596 (1976).

⁴²K. K. Berggren, R. Younkin, E. Cheung, M. Prentiss, A. J. Black, G. M. Whitesides, D. C. Ralph, C. T. Black, and M. Tinkham, *Adv. Mater.* **9**, 52 (1997).

⁴³M. Kreis, F. Lison, D. Haubrich, D. Meschede, S. Nowak, T. Pfau, and J. Mlynek, *Appl. Phys. B* **63**, 649 (1996).

⁴⁴R. Younkin, K. K. Berggren, K. S. Johnson, D. C. Ralph, M. Prentiss, and G. M. Whitesides, *Appl. Phys. Lett.* **71**, 1261 (1997).

⁴⁵P. E. Laibinis, G. M. Whitesides, D. L. Allara, Y.-T. Tao, A. N. Parikh, and R. G. Nuzzo, *J. Am. Chem. Soc.* **113**, 7152 (1991).

⁴⁶C. W. Sheen, J.-X. Shi, J. Martensson, A. N. Parikh, and D. L. Allara, *J. Am. Chem. Soc.* **114**, 1514 (1992).

⁴⁷O. S. Nakagawa, S. Ashok, C. W. Sheen, J. Martensson, and D. L. Allara, *Jpn. J. Appl. Phys., Part 1* **30**, 3759 (1991).

⁴⁸D. M. Oro, P. A. Soletsky, X. Zhang, F. B. Dunning, and G. K. Walters, *Phys. Rev. A* **49**, 4703 (1994); Y. Harada, S. Yamamoto, M. Aoki, S. Masuda, T. Ichinokawa, M. Kato, and Y. Sakai, *Nature (London)* **372**, 657 (1994); M. P. Seah and W. A. Dench, *Surf. Interface Anal.* **1**, 2 (1979).

⁴⁹K. K. Berggren, A. Bard, J. L. Wilbur, J. D. Gillaspay, A. G. Helg, J. J. McClelland, S. L. Rolston, W. D. Phillips, M. Prentiss, and G. M. Whitesides, *Science* **269**, 1255 (1995).

⁵⁰K. K. Berggren, Ph.D. thesis, Harvard University, 1996.

⁵¹S. Nowak, T. Pfau, and J. Mlynek, *Appl. Phys. B* **63**, 203 (1996).

⁵²K. G. H. Baldwin, W. Lu, D. Milic, R. M. S. Knops, M. D. Hoogerland, and S. J. Buckman, *Proc. SPIE* **2995**, 11 (1997).

⁵³A. Bard, K. K. Berggren, J. L. Wilbur, J. D. Gillaspay, S. L. Rolston, J. J. McClelland, W. D. Phillips, M. Prentiss, and G. M. Whitesides, *J. Vac. Sci. Technol. B*, these proceedings.

⁵⁴K. S. Johnson, K. K. Berggren, A. Black, C. T. Black, A. P. Chu, N. H. Dekker, D. C. Ralph, J. H. Thywissen, R. Younkin, M. Tinkham, M. Prentiss, and G. M. Whitesides, *Appl. Phys. Lett.* **69**, 2773 (1996).

⁵⁵A 1400-fold improvement in brightness was demonstrated in M. D.

- Hoogerland, J. P. J. Driessen, E. J. D. Vredenburg, H. J. L. Megens, M. P. Schuwer, H. C. W. Beijerinck, and K. A. H. van Leeuwen, *Phys. Rev. B* **62**, 323 (1996). Demonstrations of slow, bright beams include E. Riis, D. S. Weiss, K. A. Moler, and S. Chu, *Phys. Rev. Lett.* **64**, 1658 (1990) and Z. T. Lu, K. L. Corwin, M. J. Renn, M. H. Anderson, E. A. Cornell, and C. E. Wieman, *Phys. Rev. Lett.* **77**, 3331 (1996).
- ⁵⁶S. J. Rehse, A. D. Glueck, S. A. Lee, A. B. Goulakov, C. S. Menoni, D. C. Ralph, K. S. Johnson, and M. Prentiss, *Appl. Phys. Lett.* **71**, 1427 (1997).
- ⁵⁷A. P. Chu, K. K. Berggren, K. S. Johnson, and M. Prentiss, *Quantum Semiclass. Opt.* **8**, 521 (1996).
- ⁵⁸A. P. Chu, K. S. Johnson, and M. G. Prentiss, *Opt. Commun.* **134**, 105 (1997).
- ⁵⁹This absorptive grating has also been used as a detector for periodic suboptical wavelength localizations and as an optical diffraction grating for atoms. H. Batelaan, S. Bernet, M. Oberthaler, E. M. Rasel, J. Schmiedmayer, and A. Zeilinger, *Adv. At. Mol. Opt. Phys. Supplement: Atom Interferometry*, edited by P. Berman (1997).
- ⁶⁰J. E. Thomas and L. J. Wang, *Phys. Rep.* **262**, 311 (1995), and references therein.
- ⁶¹M. L. Marable, T. A. Savard, and J. E. Thomas, *Opt. Commun.* **135**, 14 (1997).
- ⁶²M. Ol'shanii, C. Herzog, N. H. Dekker, and M. Prentiss (unpublished).
- ⁶³Standard references for atomic sources include *Molecular Beams*, edited by N. F. Ramsey (Oxford University Press, Oxford, U.K., 1956, 1985) and *Atomic and Molecular Beam Methods*, edited by G. Scoles (Oxford University Press, New York, 1988).
- ⁶⁴One example is a source used for interferometry, described and measured to have a width $\Delta v/v_{mp}$ as small as 0.03 in C. R. Ekstrom, Ph.D. thesis, MIT, 1993.
- ⁶⁵T. J. Gay, *Experimental Methods in the Physical Sciences* (Academic Press, San Diego, 1996), Vol. 29B, p. 95.
- ⁶⁶D. W. Fahey, L. D. Shearer, and W. F. Parks, *Rev. Sci. Instrum.* **49**, 503 (1978).
- ⁶⁷Such sources also produce ions, electrons, and UV photons. The ions and electrons are removed by deflection plates. The photons emitted from a DC discharge source can be energetic enough to affect surfaces; in a metastable atom lithography experiment, control experiments must identify whether these UV photons are a significant component of the beam.